

A New Nanotechnology Technique for Determining Drug Efficacy Using Targeted Plasmonically Enhanced Single Cell Imaging Spectroscopy

Lauren A. Austin,[‡] Bin Kang,^{‡,†} and Mostafa A. El-Sayed*

Laser Dynamics Laboratory, School of Chemistry and Biochemistry, Georgia Institute of Technology, Atlanta, Georgia 30332-0400, United States

Supporting Information

ABSTRACT: Recently, we described a new technique, targeted plasmonically enhanced single cell imaging spectroscopy (T-PESCIS), which exploits the plasmonic properties of gold nanoparticles, e.g. gold nanospheres, to simultaneously obtain enhanced intracellular Raman molecular spectra and enhanced Rayleigh cell scattering images throughout the entire span of a single cell cycle. In the present work, we demonstrate the use of T-PESCIS in evaluating the relative efficacy and dynamics of two popular chemotherapy drugs on human oral squamous carcinoma (HSC-3) cells. T-PESCIS revealed three plasmonically enhanced Raman scattering vibration bands, 500, 1000, and 1585 cm^{-1} , associated with the cellular death dynamics. Detailed analysis indicated that the decrease in the 500 cm^{-1} band did not correlate well with drug efficacy but could indicate death initiation. The time it takes for the relative intensity of either the 1000 or 1585 cm^{-1} band (“SERS death” bands) to appear and increase to its maximum value after the injection of a known concentration of the drug can be related to the drug’s efficacy. The inverse ratio, termed cell death enhancement factor, of these characteristic death times when using either band, especially the spectrally sharp band at 1000 cm^{-1} , gave the correct drug efficacy ratio as determined by the commonly used XTT cell viability assay method. These results strongly suggest the potential future use of this technique in determining the efficacy, dynamics, and molecular mechanisms of various drugs against different diseases.

Plasmonic nanoparticles (NPs) have become exceedingly useful in medical research due to their small size and unique optical and photothermal properties.¹ By utilizing the plasmonically enhanced Rayleigh scattering from gold and silver nanospheres (Au- and AgNPs) targeted to the cell nucleus, it has been possible to distinguish between cancerous and non-cancerous cells as well as to obtain real-time cellular imaging of cancer cells during their entire cycle through cell division.² Recently, we developed a new technique, targeted plasmonically enhanced single cell imaging spectroscopy (T-PESCIS), which enables simultaneous cellular imaging and monitoring of molecular spectroscopic signals from molecules within the plasmonic fields of Au- or AgNPs targeting a cellular location, such as the nucleus, throughout the complete cell cycle, or until it

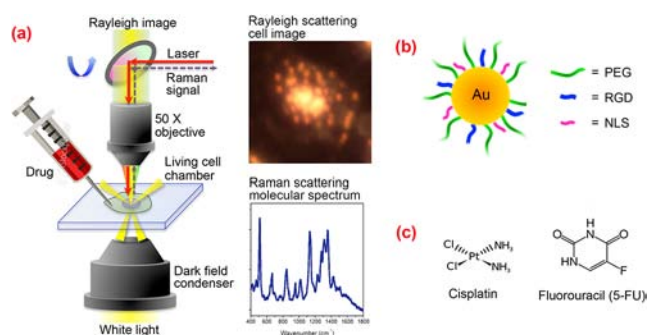


Figure 1. (a) Schematic diagram of the T-PESCIS setup used to monitor the molecular drug efficacy and dynamics of anti-cancer drugs in HSC-3 cells. (b) Illustration of the nuclear-targeted AuNPs used to enhance the Raman signals of molecules around the targeted nucleus by the AuNPs. (c) Chemical structures of the anti-cancer drugs studied.

is treated to induce cell death.³ Here we utilize this technique to study the dynamics and relative efficacy of two popular anti-cancer drugs in human oral squamous carcinoma (HSC-3) cells. The inverse ratio of the times required for each cell sample to die (i.e., the Raman bands remain unchanged with time) upon treatment with the same concentration of each drug provides the drugs’ relative efficacies.

Understanding how anti-cancer (or any anti-disease) drugs interact with cells and lead to cell death is crucial for selecting and optimizing a drug to attain the most effective treatment. A great deal of work has been done to evaluate the mechanism of action and efficacy of traditional and novel drugs by cell viability assays (i.e., XTT or MTT assays), flow cytometry, and immunoblotting.⁴ Conventionally, the standard parameters to evaluate drug efficacy have been the IC_{50} and EC_{50} , which are determined through discontinuous assays.⁵ Using T-PESCIS, we followed the time profile of cell death induced by two commonly used anti-cancer drugs to obtain information on the efficacy and dynamics of each drug. By monitoring the cellular morphology and molecular information in the form of relative Raman band intensities over time, we determined the effective time or the half-maximal effective time (ET_{50}) of the cell death process through detailed spectroscopic analysis as well as an approximate visual approach. This parameter can be used as a measure of the effectiveness of each drug in inducing cell death.

Received: January 31, 2013

Published: March 7, 2013

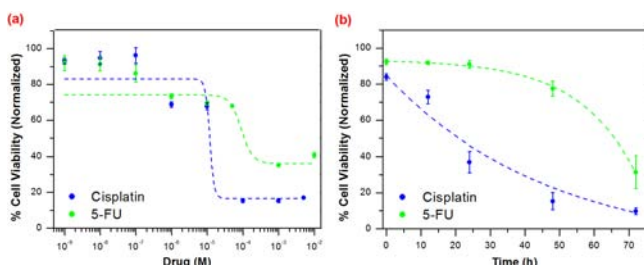


Figure 2. (a) Effective dose concentration curves of HSC-3 cells treated with increasing concentrations of cisplatin and 5-FU after 72 h treatment. EC_{50} values were calculated to be 16 μ M for cisplatin ($R^2 = 0.93$) and 89 μ M for 5-FU ($R^2 = 0.94$). (b) Time profiles of HSC-3 cells treated with 100 μ M cisplatin or 5-FU, indicating a CDE factor of 3.1.

To continuously monitor cell morphology and Raman molecular spectra over time, T-PESCIS experiments were performed on a live cell monitoring station (see Figure 1). Following the Raman spectrum over time with a homemade live cell imaging chamber allowed simultaneous acquisition of Rayleigh scattering cellular images and Raman molecular spectra from any part of a single living cell that has been targeted with a low concentration of plasmonic AuNPs (Figure 1a). The effect of drug treatment was monitored at different times after drug administration by an auto-injection system. Human oral squamous carcinoma (HSC-3) cells were used as a cancer cell model due to the overexpression of $\alpha v\beta 6$ integrins on their cellular membrane, which aid in the endocytosis of bodies that contain arginine-glycine-aspartic acid (RGD) peptides.⁶ To capture cellular images and obtain molecular information at the cell nucleus, targeted AuNSs of 24 ± 3 nm diameter were used (Figure S1). The surfaces of the AuNSs were modified to contain poly(ethylene glycol) (PEG) to ensure stability in a biological environment and reduce nonspecific binding of proteins.⁷ Following PEGylation, RGD and nuclear localizing signal (NLS) peptides were conjugated to the particle surface to exploit the overexpression of $\alpha v\beta 6$ integrins on the cell membrane and increase internalization of the particles,⁸ as well as selectively deliver the AuNSs to the cell nucleus⁹ (Figure 1b).

Drug Efficacy from the Bioanalytical Method. Two common oral anti-cancer drugs, cisplatin and 5-fluorouracil (5-FU) (Figure 1c), were chosen to determine their relative efficacy by using our T-PESCIS technique and compare it with results from other known methods.¹⁰

To test the accuracy of our method, we first determined the efficacy of each drug on our cell line by investigating the effective concentration needed to induce 50% cell death as well as monitored the time profile of cell viability vs treatment time. All experiments were performed on HSC-3 cells pretreated with 0.05 nM nuclear-targeted AuNSs to mimic the cellular system used in the T-PESCIS experiment. Using the traditional XTT cell viability assay, the EC_{50} values after treatment for 72 h were 12 μ M for cisplatin and 89 μ M for 5-FU (Figure 2a). Figure 2b displays time profiles of HSC-3 cells treated with 100 μ M of each drug over 72 h. These profiles also support the increased potency of cisplatin on HSC-3 cell viability when compared to 5-FU, as cisplatin induced 50% cell death in 21 h while 5-FU required 66 h. To concisely compare the two anti-cancer drugs, we created a new parameter called the cell death enhancement (CDE) factor, defined as the ratio of the ET_{50} of 5-FU to the ET_{50} of cisplatin calculated from the curve fits from Figure 2b. The CDE factor calculated from those time profiles was 3.1. There was no observed contribution of cell death from the targeted AuNSs

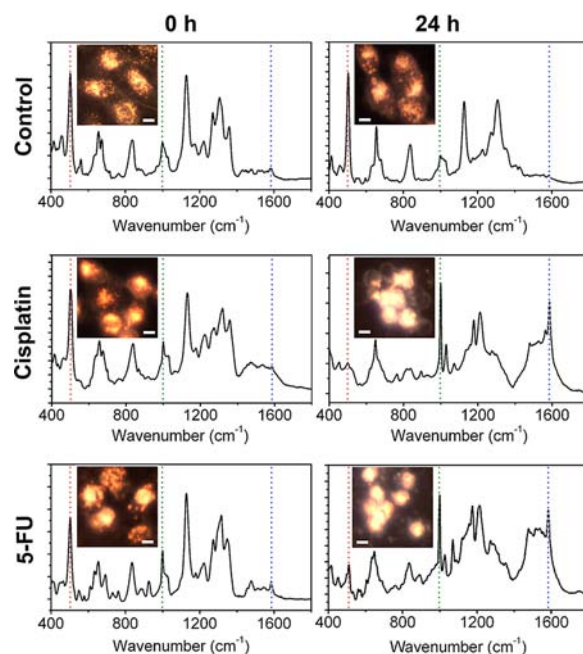


Figure 3. Representative Rayleigh images (insets, scale bar 20 μ m) and Raman spectra of HSC-3 cells before and after 24 h treatment with cisplatin and 5-FU. Distinguishable peaks, indicated by dotted lines, at 500, 1000, and 1585 cm^{-1} are used to measure cellular dynamics in response to drug treatment.

alone (Figure S2), as the obtained EC_{50} values for each drug tested are comparable to those previously reported.¹¹ The particles only enhanced the surface Raman scattering of the molecules present within the cell during treatment.

T-PESCIS Technique in Drug Efficacy Studies. Figure 3 shows the enhanced Raman spectra and Rayleigh imaging of cells before and after 24 h treatment with 100 μ M cisplatin or 5-FU. After drug treatment for 24 h, the cell morphology is significantly altered (i.e., cell shrinkage). Furthermore, the shrunken, dead cells exhibit strong white light scattering due to aggregation of cellular components as well as the cells lifting off the substrate and out of the focal plane. These visual changes suggest the occurrence of apoptotic cell death.¹² Raman spectra obtained using 785 nm laser and a low AuNS concentration (0.05 nM) show detectable changes after 24 h treatment with anti-cancer drugs, most notably a decrease in the intensity of the 500 cm^{-1} band and increases in the 1000 and 1585 cm^{-1} bands (Figure 3b,c). These Raman bands are tentatively assigned to the $-S-S-$ stretching vibration,^{13a,b} a benzene ring stretching vibration,^{13a,c-e} and a $-N-H$ out-of-plane bending vibration,^{13a,c,f-h} respectively. The latter two bands were not present in the spectra of untreated cells or the cell spectra obtained prior to anti-cancer drug treatment.

After the distinguishable changes in the three band intensities before and after drug treatment were observed, the drug action time profiles of cisplatin and 5-FU on HSC-3 cells were investigated using the T-PESCIS technique to determine its accuracy in evaluating a drug's efficacy and dynamics of single cell death (Figure 4). Although the observed spectral changes after administration of the two drugs were similar, the times after injection at which the intensity of these bands begins to change, as well as the rates of their change, were markedly different. 5-FU required more time to show changes in the intensity of the three main bands. The increase in time required for 5-FU to display the

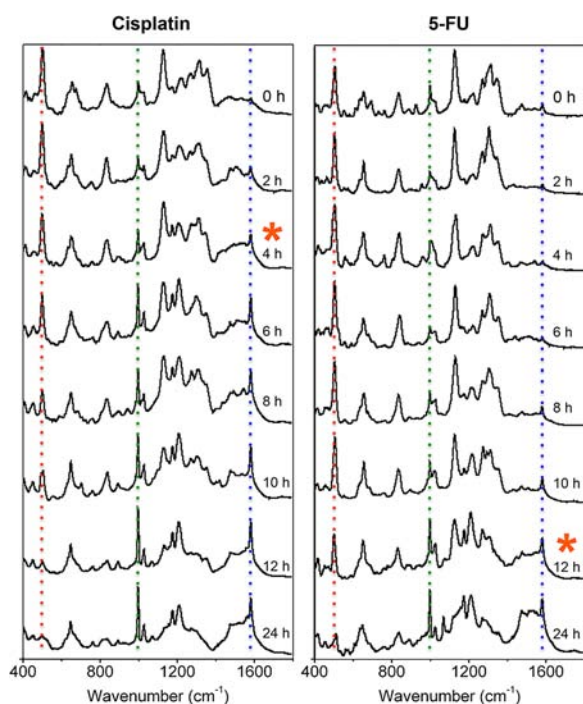


Figure 4. Real-time Raman spectra of HSC-3 cells treated for 24 h with cisplatin and 5-FU. The identified “spectroscopic death initiation” band is at 500 cm^{-1} , while the “SERS death” bands are at 1000 and 1585 cm^{-1} . The stars indicate when the spectra remain constant.

changes in band intensity agrees with the cell viability trends described above. Since the peak around 500 cm^{-1} decreases over time and most likely corresponds to disulfide bond dissociation within highly structured proteins,^{13b} we called this the “spectroscopic death initiation” (SDI) band. We designated the bands at 1000 and 1585 cm^{-1} “SERS death” (SD) bands, since it is believed that these bands appear as more proteins and/or DNA fragments become exposed to the AuNSs’ surface plasmon field as the cell dies. The 1000 cm^{-1} band may correspond to the benzene ring stretching vibration of phenylalanine.^{13c-e} While there are varying reports on the identification of the band 1585 cm^{-1} , we tentatively assign it to the $-\text{N}-\text{H}$ bending vibration of guanine or adenine residues within DNA.^{13c,f-h} As it is known that both cisplatin and 5-FU cause cell death through an apoptotic mechanism,¹⁴ it is possible that once apoptosis is triggered, the DNA begins to fragment, losing its double-stranded feature and allowing the $-\text{NH}$ groups to be exposed to the plasmon field of the nuclear-targeted AuNSs.¹⁵

Relative Drug Efficacy from Detailed T-PESCIS Analysis. To further understand the anti-cancer drugs’ dynamics, we analyzed the relative band intensity changes over time for the SDI band at 500 cm^{-1} and the SD bands at 1000 and 1585 cm^{-1} (Figure 5). We fit the intensities of all three death-sensitive bands to a sigmoidal growth function. The ET_{50} values for cisplatin and 5-FU, calculated from the sigmoidal growth fit for each band, were used to compare the efficacy of the two drug molecules (see Figure 5d). Although the ET_{50} ’s obtained for these bands do not correspond numerically to those determined using the traditional XTT cell viability assays, the trends and CDE factors are similar. The CDE factors were calculated to be 1.9, 3.4, and 3.3 for the 500 , 1000 , and 1585 cm^{-1} bands, respectively. The bands at 1000 and 1585 cm^{-1} provided CDE factors that correlated well with those obtained from the bioanalytical technique. The poor agreement between the CDE factors when using the 500 cm^{-1}

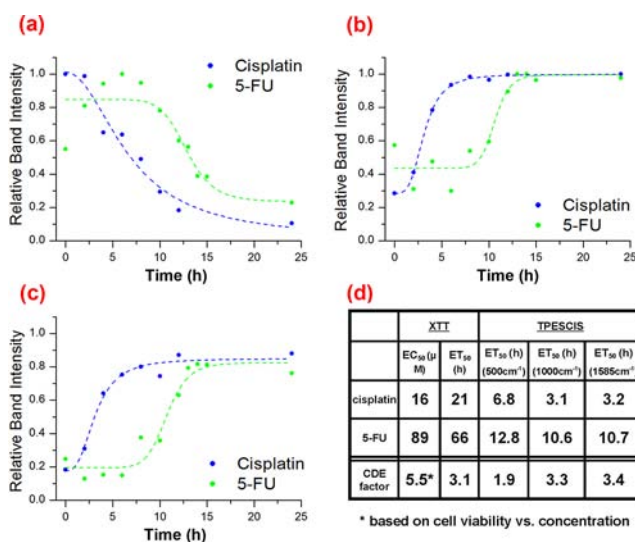


Figure 5. Time profiles of three Raman bands used to monitor the transition from live to dead HSC-3 cells after treatment with cisplatin or 5-FU. SDI and SD bands centered at (a) 500 , (b) 1000 , and (c) 1585 cm^{-1} indicate CDE factors of 1.9, 3.4, and 3.3, respectively. The CDE factors of the 1000 and 1585 cm^{-1} bands obtained with the T-PESCIS method are comparable to those obtained by the standard XTT assay (d).

band and its continuous change in intensity after the rest of the spectrum remained unchanged (due to cell death) indicated this band should not be used to assess drug efficacy. For this new technique, a spectrally sharp and highly resolved band, like the 1000 cm^{-1} band that stops changing in intensity along with the majority of the spectrum, should be selected for accurate determination of the cell viability and thus of the efficacy in the systems being studied. It should be mentioned that different systems (i.e., cell lines, treatments, etc.) could reveal different spectrally sharp bands that should be utilized.

Relative Drug Efficacy from Direct Visual Inspection Using T-PESCIS Spectroscopic Analysis. A rapid, easy, and approximate method using T-PESCIS to determine the relative efficacy of two drugs was also investigated. Comparing the SERS spectra as a function of time for the two drugs, at the same known concentration, gave CDE factors similar to those obtained with our detailed T-PESCIS analysis. The time required for the intensity of the majority of the bands in the spectrum, especially of the SD bands, to become constant was determined, and these characteristic times were used to evaluate the relative efficacies of cisplatin and 5-FU. The determined times, as indicated by the orange stars in Figure 4, were 4 and 12 h for cisplatin and 5-FU, respectively. The inverse ratio of these characteristic times, or CDE factor, was calculated to be ~ 3 , comparable to that determined from the detailed method described above. Naturally, following the relative intensity changes of the spectrally sharp bands, such as those at 1000 or 1585 cm^{-1} , should provide a more accurate determination of cell death, particularly if the time between sequential spectra is reduced (i.e., 0.5 vs 2.0 h). From the inverse death time ratio and the known ET_{50} of the standard, the ET_{50} value of the unknown drug can be calculated.

In both T-PESCIS methods discussed above, a drug with known efficacy must be used as a standard. This standard drug will vary with the type of cancer or disease as well as the cell line being examined. To utilize this method correctly, several procedural steps must be followed: (1) The chosen cell line

must be treated with a concentration of AuNSs that does not perturb normal functionality of the cells, but still provides an enhanced Raman signal (i.e., 0.05 nM NLS/RGD-AuNSs from this work). (2) The plasmonic NP and its aggregate must be strongly localized to the region of the cell that provides the best signals for cell death (i.e., the nucleus). (3) The sharpest and most highly resolved band observed in both drug treatments, whose intensity signifies death, must be identified and analyzed over time (i.e., 1000 cm^{-1} in the present work). (4) In the detailed T-PESCIS method, the chosen band must be normalized to the most intense band in the spectra over time and fit with a model that correlates best for the treatments being examined, and the comparison of efficacy should be based on the calculated ET_{50} values. Although this new method follows steps similar to traditional XTT cell viability assays, the T-PESCIS technique required 3 days of preparation and analysis on the molecular scale, while the XTT assay required 5 days of preparation and analysis to attain a similar CDE factor (Figures 2 and 5).

In conclusion, we have demonstrated the use of T-PESCIS to study and characterize the relative drug efficacy and dynamics of two popular oral anti-cancer drugs. This new method has the ability to evaluate the time profile and efficacy of a drug in real time without needing to prepare multiple samples. While this setup is currently limited to macroscale sample holders, it could be engineered into a microplate scale, allowing for sensitive and real-time detection of multiple drugs at one time, as well as the ability to obtain spectra from a larger population of cells to obtain more statistically assured results. Additionally, this new method has the potential to provide new fundamental insight into the interaction of drugs and living cells, as well as to offer a spectroscopic method that can determine the cell death mechanisms induced by different drugs. These findings could ultimately be used in selecting a drug of choice for particular patients with different types of cancer or other diseases.

■ ASSOCIATED CONTENT

Supporting Information

Experimental details, TEM, and UV–vis and Raman spectra. This material is available free of charge via the Internet at <http://pubs.acs.org>.

■ AUTHOR INFORMATION

Corresponding Author

melsayed@gatech.edu

Author Contributions

[‡]L.A.A. and B.K. contributed equally.

Notes

The authors declare no competing financial interest.

[†]Permanent address for B.K.: College of Material Science and Technology, Nanjing University of Aeronautics and Astronautics, Nanjing 210016, P.R. China.

■ ACKNOWLEDGMENTS

The authors acknowledge Megan A. Mackey for taking TEM images of the AuNSs.

■ REFERENCES

(1) (a) Huang, X.; El-Sayed, I. H.; Qian, W.; El-Sayed, M. A. *J. Am. Chem. Soc.* **2006**, *128*, 2115. (b) Jain, K. K. *BMC Med.* **2010**, *8*, 1. (c) Jain, P. K.; Huang, X.; El-Sayed, I. H.; El-Sayed, M. A. *Acc. Chem. Res.* **2008**, *41*, 1578. (d) Jans, H.; Huo, Q. *Chem. Soc. Rev.* **2012**, *41*, 2849.

(e) Huang, X.; Jain, P.; El-Sayed, I.; El-Sayed, M. *Lasers Med. Sci.* **2008**, *23*, 217. (f) Liao, H.; Nehl, C. L.; Hafner, J. H. *Nanomedicine* **2006**, *1*, 201.

(2) (a) Kang, B.; Mackey, M. A.; El-Sayed, M. A. *J. Am. Chem. Soc.* **2010**, *132*, 1517. (b) Austin, L. A.; Kang, B.; Yen, C.-W.; El-Sayed, M. A. *Bioconjugate Chem.* **2011**, *22*, 2324.

(3) Kang, B.; Austin, L. A.; El-Sayed, M. A. *Nano Lett.* **2012**, *12*, 5369.

(4) (a) Irwin, M. S.; Kondo, K.; Marin, M. C.; Cheng, L. S.; Hahn, W. C.; Kaelin, W. G., Jr. *Cancer Cell* **2003**, *3*, 403. (b) Wu, S.-J.; Ng, L.-T. *Food Chem. Toxicol.* **2007**, *45*, 2446. (c) Lim, E.-S.; Rhee, Y.-H.; Park, M.-K.; Shim, B.-S.; Ahn, K.-S.; Kang, H. E. E.; Yoo, H.-S.; Kim, S.-H. *Ann. N.Y. Acad. Sci.* **2007**, *1095*, 7. (d) Li, L.; Yue, G. G. L.; Lau, C. B. S.; Sun, H.; Fung, K. P.; Leung, P. C.; Han, Q.; Leung, P. S. *Toxicol. Appl. Pharmacol.* **2012**, *262*. (e) Citro, G.; D'Agnano, I.; Leonetti, C.; Perini, R.; Bucci, B.; Zon, G.; Calabretta, B.; Zupi, G. *Cancer Res.* **1998**, *58*, 283. (f) Etienne, M. C.; Bernard, S.; Fischel, J. L.; Formento, P.; Gioanni, J.; Santini, J.; Demard, F.; Schneider, M.; Milano, G. *Br. J. Cancer* **1991**, *63*, 372.

(5) (a) Bocci, G.; Nicolaou, K. C.; Kerbel, R. S. *Cancer Res.* **2002**, *62*, 6938. (b) Andreotti, P. E.; Cree, I. A.; Kurbacher, C. M.; Hartmann, D. M.; Linder, D.; Harel, G.; Gleiberman, I.; Caruso, P. A.; Ricks, S. H.; Untch, M.; Sartori, C.; Bruckner, H. W. *Cancer Res.* **1995**, *55*, 5276. (c) Ulukaya, E.; Ozdikicioglu, F.; Oral, A. Y.; Demirci, M. *Toxicol. In Vitro* **2008**, *22*, 232.

(6) (a) Takayama, S.; Hatori, M.; Kurihara, Y.; Shirota, T.; Shintani, S. *Oncol. Rep.* **2009**, *21*, 205. (b) Xue, H.; Atakilit, A.; Zhu, W.; Li, X.; Ramos, D. M.; Pytela, R. *Biochem. Biophys. Res. Commun.* **2001**, *288*, 610.

(7) Wuelfing, W. P.; Gross, S. M.; Miles, D. T.; Murray, R. W. *J. Am. Chem. Soc.* **1998**, *120*, 12696.

(8) (a) Busk, M.; Pytela, R.; Sheppard, D. *J. Biol. Chem.* **1992**, *267*, 5790. (b) Dehari, H.; Ito, Y.; Nakamura, T.; Kobune, M.; Sasaki, K.; Yonekura, N.; Kohama, G.; Hamada, H. *Cancer Gene Ther.* **2003**, *10*, 75.

(9) Dingwall, C.; Laskey, R. A. *Trends Biochem. Sci.* **1991**, *16*, 478.

(10) (a) Andreadis, C.; Vahtsevanos, K.; Sidiras, T.; Thomaidis, I.; Antoniadis, K.; Mouratidou, D. *Oral Oncol.* **2003**, *39*, 380. (b) Go, R. S.; Adjei, A. A. *J. Clin. Oncol.* **1999**, *17*, 409. (c) Kim, E.; Glisson, B. *Cancer Treat. Res.* **2003**, *114*, 295.

(11) (a) Torre, C.; Wang, S. J.; Xia, W.; Bourguignon, L. Y. *Arch. Otolaryngol., Head Neck Surg.* **2010**, *136*, 493. (b) Sato, T.; Suzuki, M.; Sato, Y.; Echigo, S.; Rikiishi, H. *Int. J. Oncol.* **2006**, *28*, 1233. (c) Masuda, M.; Suzui, M.; Weinstein, I. B. *Clin. Cancer Res.* **2001**, *7*, 4220.

(12) (a) Gerschenson, L.; Rotello, R. *FASEB J.* **1992**, *6*, 2450. (b) Austin, L. A.; Kang, B.; Yen, C.-W.; El-Sayed, M. A. *J. Am. Chem. Soc.* **2011**, *133*, 17594.

(13) (a) Peticolas, W. L. *Methods in Enzymology*; Academic Press: San Diego, 1995; Vol. 246. (b) Zheng, R.; Zheng, X.; Dong, J.; Carey, P. R. *Protein Sci.* **2004**, *13*, 1288. (c) Puppels, G. J.; de Mul, F. F. M.; Otto, C.; Greve, J.; Robert-Nicoud, M.; Arndt-Jovin, D. J.; Jovin, T. M. *Nature* **1990**, *347*, 301. (d) Wu, H.; Volponi, J. V.; Oliver, A. E.; Parikh, A. N.; Simmons, B. A.; Singh, S. *Proc. Natl. Acad. Sci. U.S.A.* **2011**, *108*, 3809. (e) Culka, A.; Jehlička, J.; Edwards, H. G. M. *Spectrochim. Acta, Part A* **2010**, *77*, 978. (f) Shanmugasundaram, M.; Puranik, M. *Phys. Chem. Chem. Phys.* **2011**, *13*, 3851. (g) Hud, N. V.; Milanovich, F. P.; Balhorn, R. *Biochemistry* **1994**, *33*, 7528. (h) Deng, H.; Bloomfield, V. A.; Benevides, J. M.; Thomas, G. J. *Biopolymers* **1999**, *50*, 656.

(14) (a) Guchelaar, H. J.; Vermees, I.; Koopmans, R. P.; Reutelingsperger, C. P.; Haanen, C. *Cancer Chemother. Pharmacol.* **1998**, *42*, 77. (b) Matsushashi, N.; Saio, M.; Matsuo, S.; Sugiyama, Y.; Saji, S. *Int. J. Oncol.* **2005**, *26*, 1563.

(15) (a) Elmore, S. *Toxicol. Pathol.* **2007**, *35*, 495. (b) Ikeda, M.; Kurose, A.; Takatori, E.; Sugiyama, T.; Traganos, F.; Darzynkiewicz, Z.; Sawai, T. *Int. J. Oncol.* **2010**, *36*, 1081.